

We are IntechOpen, the world's leading publisher of Open Access books Built by scientists, for scientists

6,900

Open access books available

186,000

International authors and editors

200M

Downloads

Our authors are among the

154

Countries delivered to

TOP 1%

most cited scientists

12.2%

Contributors from top 500 universities



WEB OF SCIENCE™

Selection of our books indexed in the Book Citation Index
in Web of Science™ Core Collection (BKCI)

Interested in publishing with us?
Contact book.department@intechopen.com

Numbers displayed above are based on latest data collected.
For more information visit www.intechopen.com



Synchronous Vapor-Phase Coating of Conducting Polymers for Flexible Optoelectronic Applications

Keon-Soo Jang and Jae-Do Nam
Sungkyunkwan University
Republic of Korea

1. Introduction

Since conducting polymers (CP) were first reported, poly(3,4-ethylenedioxythiophene) (PEDOT) is arguably one of the most commercially useful and most studied CPs in the last 20 years (Shirakawa et al., 1977; Chiang et al., 1977; Winther-Jensen et al., 2007; Truong et al., 2007). PEDOT has been studied extensively on account of its many advantageous properties, such as high electrical conductivity, good transmittance and thermal stability with a low optical bandgap and thermal stability (Winther-Jensen & West, 2004; Jonas et al., 1991). These properties make PEDOT very attractive for applications, such as electrochromic windows (Welsh et al., 1999), organic electrodes for organic photovoltaic cells (OPVs) (Admassie et al., 2006; Gadisa et al., 2006) and hole injection layers (HIL) in organic light emitting devices (OLEDs) (Wakizaka et al., 2004; Hatton et al., 2009) and dye-sensitized solar cells (Saito et al., 2005). In particular, PEDOT is commonly used as a hole extraction layer in OPVs (Colladet et al., 2007; Kim et al., 2005). In most optoelectronic applications as a buffer or electrode layer, the bandgap of the layer plays an important role in determining the operating characteristics, quantum efficiency and electron/hole transport. Therefore, the main issues for electronic device applications include both the electrical conductivity and bandgap.

Oxidized PEDOT can be produced in a variety of forms using different polymerization techniques. Solution processing is used most commonly in synthesizing PEDOT in the form of spin-coating, solvent-casting or ink-jet printing. However, these PEDOT systems are relatively insoluble in most solvents, making it necessary to attach soluble functional groups to the polymer or dope it with stabilizing polyelectrolytes (Terje & Skotheim, 1998). An aqueous dispersion of poly(3,4-ethylenedioxythiophene)-poly(styrenesulfonate) (PEDOT-PSS), commercially available as Baytron P, is a stable polymer system with a high transparency up to 80% (Groenendaal et al., 2000). However, the PEDOT-PSS film exhibits relatively low electrical conductivity, 10-500 S/cm (Groenendaal et al., 2000), which does not often meet the high conductivity required for most applications. In addition, scanning-tunneling microscopy, neutron reflectivity measurements, and x-ray photoelectron spectroscopy have revealed a PSS rich layer on the top of the spin-coated PEDOT-PSS films due to the phase separation (Lee & Chung, 2008; Kemerink et al., 2004; Higgins et al., 2003). Since PSS is an electrical insulator, excessive PSS can limit the film conductivity (Kemerink

et al., 2004), and an acidic PEDOT-PSS dispersion can etch indium tin oxide (ITO) during the polymer spin-coating process. Moreover, the hydrolysis of the deposited PEDOT-PSS by moisture absorption can also etch ITO to cause indium and tin incorporation into the polymer (Lee et al., 2007).

For the PEDOT systems without using polyelectrolytes, PEDOT can be deposited directly on the substrate surface by several in-situ polymerization techniques. One of the options is electrochemical polymerization, which has been reported to have higher electrical conductivity (Groenendaal et al., 2001). However, electrochemical polymerization results in a poor transparency and requires conducting substrates, which limits its practical applications. As an alternative, oxidative chemical polymerization either in the liquid or vapor phase is more versatile because it is not restricted by the substrates. In particular, one way of achieving a clear thin film with a smooth surface is to apply the oxidant using solvent coating processes and expose the coated surface to a reactive monomer vapor. This process is often referred to as vapor phase polymerization (referred to herein as VPP) (Kim et al., 2003; Fabretto et al., 2008; Cho et al., 2008; Ha et al., 2004; Winther-Jensen et al., 2004). The PEDOT films by VPP have been reported to have conductivities of approximately 15 S/cm at a thickness of 300 nm without any additives (Kim et al., 2003). Recently, a PEDOT film with high conductivity, exceeding 1000 S/cm, was reported using a base-inhibited VPP (Winther-Jensen et al., 2007). However, it should be noted that VPP PEDOT has a high bandgap and relatively low transmittance (Fabretto et al., 2008; Cho et al., 2008).

As another thiophene-based conducting polymer, poly(3-hexylthiophene) (P3HT) is also one of the most indispensable materials in OLEDs, OPVs, field effect transistors (FETs) and thin film transistors (TFTs) (Hatton et al., 2009; Kim et al., 2005; Grecu et al., 2006; Bartic et al., 2002). Over the last decade, blending or copolymerization techniques of conducting polymers have been investigated not only to overcome the drawbacks of a pristine conductive polymer, such as inadequate bandgap, rough surface, low conductivity and poor transmittance, but also to tailor the properties for various applications (Kim et al., 2009; Xu et al., 2006; Sarac et al., 2003). This study investigated P3HT thin films deposited using a vapor-phase polymerization (VPP) technique (Ha et al., 2004; Winther-Jensen et al., 2004), which desirably ensures thin film formation in various substrate materials without the additional processes to liquefy polymers (Jang et al., 2009). It is believed that the VPP technique for P3HT will allow the fabrication of thin coatings over a large surface area of various substrate materials. We used a similar route to VPP of PEDOT choosing appropriate catalyst and solvent systems. Using the VPP technique, therefore, PEDOT and P3HT may be copolymerized in the state of vaporized monomers and subsequently polymerized to form, most probably, a PEDOT/P3HT copolymer structure. However, it should be mentioned that the traditional VPP route, where the monomer is maintained in the state of thermodynamic equilibrium, may not simply be applied because the vapor pressure and polymerization rate of the EDOT and 3HT are different and, thus, the relative composition of the VPP copolymer is not controllable (Jang et al., 2010).

Therefore, the PEDOT to P3HT ratio was kinetically controlled in this study by adjusting the relative feed amount of the evaporating monomers to the reaction chamber to fabricate the PEDOT/P3HT films containing different ratios of PEDOT to P3HT. The developed synchronous VPP technique successfully provided PEDOT/P3HT copolymer thin coatings with tunable bandgap and optoelectronic properties.

2. Conducting polymers

2.1 Summary of conducting polymers

Conducting polymers—plastics that conduct electricity—continue to find market niches in consumer electronics and antistatic textiles, some of which have military applications. Among the most exciting applications is the use of conducting polymers in light-emitting devices (LEDs), replacing silicon as the traditional substrate material for clock radios, audio equipment, televisions, cellular telephones, automotive dashboard displays, and aircraft cockpit displays. Conducting polymers provide benefits to industries such as electronics by shielding against electromagnetic interference (EMI). Conductive polymers are also already used in devices that detect environmentally hazardous chemicals, factory emissions, and flavors or aromas in food products. Currently, their conductivity is being explored in electrostatic materials, conducting adhesives, electromagnetic shielding, artificial nerves, aircraft structures, diodes, and transistors.

2.2 Correlation of chemical structure and electrical conductivity

In traditional polymers such as polyethylenes, the valence electrons are bound in sp^3 hybridized covalent bonds. Such "sigma-bonding electrons" have low mobility and do not contribute to the electrical conductivity of the material. The situation is completely different in conjugated materials. Conducting polymers have backbones of contiguous sp^2 hybridized carbon centers. One valence electron on each center resides in a p_z orbital, which is orthogonal to the other three sigma-bonds. The electrons in these delocalized orbitals have high mobility when the material is "doped" by oxidation, which removes some of these delocalized electrons. Thus the p -orbitals form a band, and the electrons within this band become mobile when it is partially emptied. In principle, these same materials can be doped by reduction, which adds electrons to an otherwise unfilled band. In practice, most organic conductors are doped oxidatively to give p -type materials. The redox doping of organic conductors is analogous to the doping of silicon semiconductors, whereby a small fraction silicon atoms are replaced by electron-rich (e.g., phosphorus) or electron-poor (e.g. boron) atoms to create n -type and p -type semiconductors, respectively.

Although typically "doping" conductive polymers involves oxidizing or reducing the material, conductive organic polymers associated with a protic solvent may also be "self-doped."

The most notable difference between conductive polymers and inorganic semiconductors is the mobility, which until very recently was dramatically lower in conductive polymers than their inorganic counterparts. This difference is diminishing with the invention of new polymers and the development of new processing techniques. Low charge carrier mobility is related to structural disorder. In fact, as with inorganic amorphous semiconductors, conduction in such relatively disordered materials is mostly a function of "mobility gaps" with phonon-assisted hopping, polaron-assisted tunneling, etc., between localized states.

The conjugated polymers in their undoped, pristine state are semiconductors or insulators. As such, the energy gap can be > 2 eV, which is too great for thermally activated conduction. Therefore, undoped conjugated polymers, such as polythiophenes, polyacetylenes only have a low electrical conductivity of around 10^{-10} to 10^{-8} S/cm. Even at a very low level of doping ($< 1\%$), electrical conductivity of increases several orders of magnitude up to values of around 0.1 S/cm. Subsequent doping of the conducting polymers will result in a saturation of the conductivity at values around 0.1–10 kS/cm for different polymers. Highest values

reported up to now are for the conductivity of stretch oriented polyacetylene with confirmed values of about 80 kS/cm. Although the pi-electrons in polyacetylene are delocalized along the chain, pristine polyacetylene is not a metal. Polyacetylene has alternating single and double bonds which have lengths of 1.44 and 1.36 Å, respectively. Upon doping, the bond alteration is diminished in conductivity increases. Non-doping increases in conductivity can also be accomplished in a field effect transistor (organic FET or OFET) and by irradiation. Some materials also exhibit negative differential resistance and voltage-controlled "switching" analogous to that seen in inorganic amorphous semiconductors.

2.3 Synthesis of conducting polymer

Chemical, oxidative coupling, electrochemical, chemical oxidative, Grignard polycondensation, and quasi-living polymerization are commonly used. In chemical oxidative polymerization, a monomer, oxidizing agent, and a dopant are reacted on the dielectric surfaces to form the conductive polymer. In electrochemical polymerization, conducting polymers such as Polypyrrole and Polyaniline films of uniform morphology and good electrical conductivity are formed on Indium Tin Oxide glass electrodes in supercritical CO₂ where the only added ingredient is electrolyte dopant. Furthermore, conducting polymers are chemically polymerized in an aqueous medium to which an oxidant is added. Sometimes, in addition to the ingredients, a protonic acid is added to the aqueous polymerization mixture that renders the final polymers conductive. The oxidative polymerization of monomers to obtain conductive polymer is affected by the oxidation potential level of monomer as well as the oxidizing capability of oxidizing agent. In the example of Fe (III) oxidizing agent, the Fe (III) ion would form a complex with a specific compound having lone pair electrons, which alters the oxidizing strength of Fe (III) ion. The stronger the complex bonding is, the lower the oxidizing capability of the oxidizing agent is.

3. Fabrication of the VPP conducting polymers

3.1 VPP-P3HT

The substrates were washed and rinsed with DI-water and acetone while being sonicated for 10 minutes to remove any organic contaminants. The glass substrates plasma treated (KSC Korea switching, Korea) for 10 minutes (10 kHz & 10 V & 7 A at a speed of 50 cc Helium/min), and the ITO glass substrates were UV-treated for 20 min. The catalyst was a mixture of MeOH and EtOH at 1:1 ratio with FeCl₃•6H₂O. After sonicating the catalyst solution for 2 minutes at 40°C, it was spin-coated onto the substrates at a speed of 500 rpm for 5 seconds and then at 1400 rpm for 5 seconds. Subsequently, the catalyzed substrates were placed in the vapor-phase-polymerization (VPP) chamber containing 3-hexylthiophene (3HT) monomer to evaporate and fill therein under a nitrogen purge, which is similar to that reported elsewhere (Truong et al., 2008). The 3HT monomers in the VPP chamber were polymerized for one hour at 50°C. The sample was soaked and washed sequentially with MeOH to eliminate the monomers remaining on the substrate. The washed P3HT film was further dried to remove the residual solvents for 10 minutes in ambient atmosphere.

3.2 VPP-P3HT/PEDOT copolymers

The substrates were washed and rinsed with DI-water and acetone and sonicated for 10 minutes to remove any organic contaminants. The glass substrates were plasma-treated

(PLAMAX, SPS Co., Ltd., Korea) for 30 seconds, and the ITO glass substrates were UV-treated for 20 minutes. The oxidant was a mixture of MeOH and EtOH at a 1:1 ratio with iron (III) chloride hexahydrate. The wt% ratio between the alcohol mixture and $\text{FeCl}_3 \cdot 6\text{H}_2\text{O}$ was 10:1, 5:1, and 3:1. A ratio of 10:1 was chosen to fabricate most thin films in this study. After sonicating the oxidant solution for 2 minutes at 40°C , it was spin-coated onto the substrates at a speed of 500 rpm for 5 seconds and then at 1400 rpm for 5 seconds. The oxidized substrates were placed in the vapor-phase-polymerization (VPP) chamber, where the containers of 3HT and EDOT were also placed. The vaporized monomers were supplied into the chamber through the feed inlets, which were made at the center of the container ceiling with different inlet diameters of D_{3HT} and D_{EDOT} (Scheme 1). The flow rate of flowing nitrogen was kept constant during polymerization, and the feed ratio of 3HT and EDOT monomer vapors was adjusted by the inlet diameters of D_{3HT} (0, 2, 4, 6, and 8 mm) and D_{EDOT} (fixed at 20 mm). The EDOT and 3HT monomers in the VPP chamber were polymerized for 20 min, 30 min, or 1 hour at 60°C . After polymerization, the sample was soaked and washed sequentially with MeOH to eliminate the monomers and Fe(III) solution remaining on the substrate. The washed PEDOT/P3HT copolymer film was dried further using a hot-air gun for 1 minute in an ambient atmosphere to remove the residual MeOH.

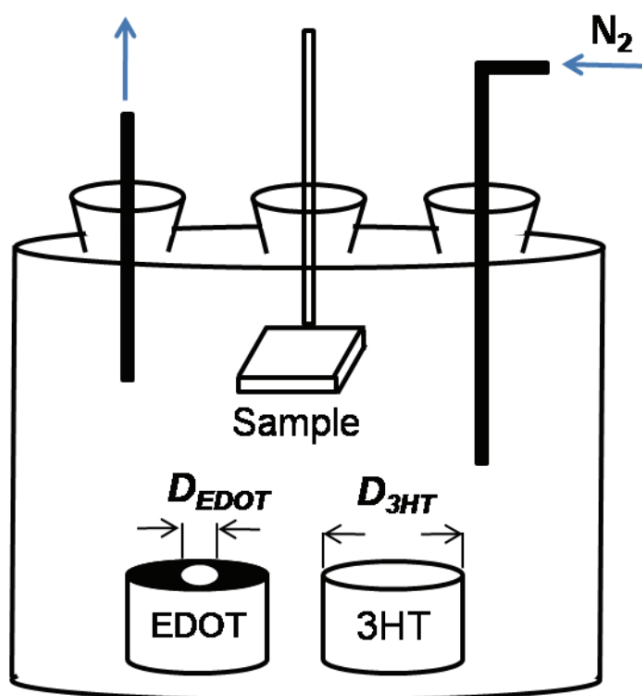


Fig. 1. Schematic of experimental setup for synchronous polymerization of EDOT and 3HT monomers, where the monomer concentrations are controlled by the inlet sizes of monomers (D_{EDOT} and D_{3HT}) to the reaction chamber under the flowing inert gas

4. Measurement

The thickness of the VPP PEDOT/P3HT was measured using an alpha step IQ (KLA Tencor corporate, the Yield Management company, San Jose CA, U.S.A.) and FE-SEM (Field emission scanning electron microscope, 1.0nm guaranteed at 15kV, JSM6700F, JEOL, Japan). The bandgap was determined by UV-vis-spectrophotometry (UV-3600, SHIMADZU,

Japan). AFM (SPA-300HV, SII Nano Technology Inc. Tokyo Japan) was used to examine the surface morphology of the VPP-PEDOT/P3HT coating, where a $5\ \mu\text{m} \times 5\ \mu\text{m}$ area was analyzed to determine the surface roughness. The AFM 3D images revealed the surface roughness of the copolymer films with a z-axis of 100 nm. X-ray photoelectron spectroscopy (XPS, ESCA2000, VG MICROTECH) equipped with an Al K α radiation source ($h\nu = 1486.6\ \text{eV}$) was used to analyze the components. Attenuated total reflection-Fourier transform infrared (ATR-FTIR) spectroscopy (Bruker IFS-66/S, Bruker, Massachusetts U.S.A.) was also used for component analysis of the VPP-PEDOT/P3HT copolymers. Contact angle measurements were performed using a Digi-drop contact angle goniometer (JinTech, Korea). A water droplet was dropped onto the surface of a small sample. The droplet shape was recorded by a camera and analyzed to determine the contact angle. The electrical conductivity of the synthesized films was measured using a four-point probe method (Keithley 236 current source and Keithley 617 electrometer). The film thickness for the measurement of electrical conductivities ranged 100 – 500 nm coated on a glass substrate in the area of $25 \times 25\ \text{mm}^2$. The type of the four-probe point was a linear type with 1 mm tip spacing. The HOMO (highest occupied molecular orbital) was measured using an ultraviolet photoelectron spectrometer (UPS, Surface Analyzer, Model AC-2, Riken-Keiki Co., Japan). The molecular weight of VPP-P3HT was measured by the matrix-assisted laser desorption ionization mass spectrometer (MALDI-MS, Voyager-DE STR biospectrometry Workstation, Applied Biosystems Inc.) equipped with N₂ UV-laser radiating at 337 nm wavelength using THF as a solvent and dithranol as a matrix.

5. Optical properties - bandgap

5.1 VPP-P3HT

Fig. 2 shows the UV-vis transmittance spectra of a VPP-P3HT film formed on a glass substrate after being polymerized at 50 °C for 1 hour. Taking the isobestic point at 650 nm as the energy gap, the band gap was estimated to be 1.91 eV, which is similar to that of conventional polythiophenes corresponding to the 70% regioregular head-to-tail (HT) P3HT

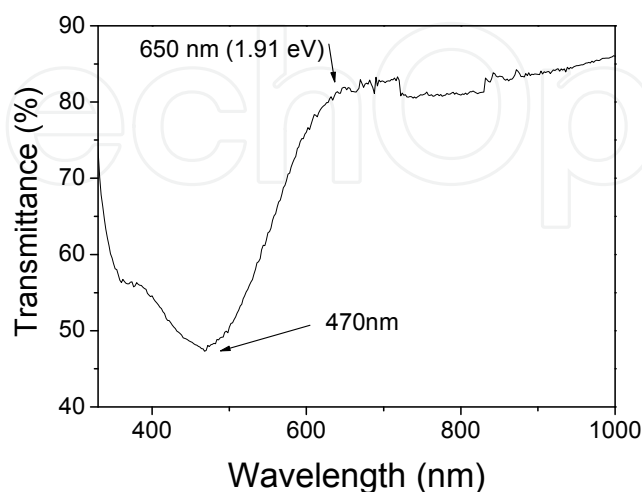


Fig. 2. UV-vis spectrum of the P3HT thin coating formed at 50 °C 1 hour

case (Chen et al., 1995; Chan et al., 1998). The measured value in this study is believed to be a proper band gap in OLED and photovoltaic cells (Li et al., 2004; Du Pasquier et al., 2005). The regioregularity of P3AT is also considered to be extremely important for the manifold properties, such as conductivity and the extent of crystal growth (McCullough, 1998; Skotheim & Reynolds, 2007; Chan et al., 1998). The regioregular head-to-tail P3ATs form well-defined and well-organized 3D structures in the form of π -stacks, which usually lead to both better material characteristics and enhanced device performance in almost all categories ranging from electrical conductivity to stability (Li et al., 2004; Du Pasquier et al., 2005). The minimum peak (λ_{\min}) at 470 nm in Fig. 2 indicates the regioregularity of P3HT corresponding to a 70% rr-P3HT of the π - π^* transition (Chen et al., 1995; Chan et al., 1998).

5.2 VPP-P3HT/PEDOT copolymers

Fig. 3 presents the UV-vis absorbance spectra of VPP-PEDOT/P3HT films on glass substrates leading to changes of the bandgap of the VPP-PEDOT/P3HT copolymer at different feed ratio of r values. The bandgap was estimated to be 1.91, 1.98, 2.02, 2.07, and 2.16 eV for the specimens prepared with 0, 2, 4, 6 mm of feed diameters and the pristine VPP-PEDOT film, respectively, by taking the isobestic points at 650, 625, 615, 600, and 575 nm, respectively. The bandgap decreases gradually with decreasing EDOT monomer supply. Accordingly, the bandgap of the VPP-PEDOT/P3HT copolymer film can be desirably adjusted by changing the relative composition of PEDOT and P3HT, especially when a low bandgap is required in such applications as OLEDs and OPVs (Colladet et al., 2007). The inset in Fig. 3 shows the pristine PEDOT, P3HT and PEDOT/P3HT copolymers at different compositions coated on glass substrates. The color of the specimens clearly indicates that the compositions of PEDOT and P3HT vary with the fabrication conditions to give tunable bandgap.

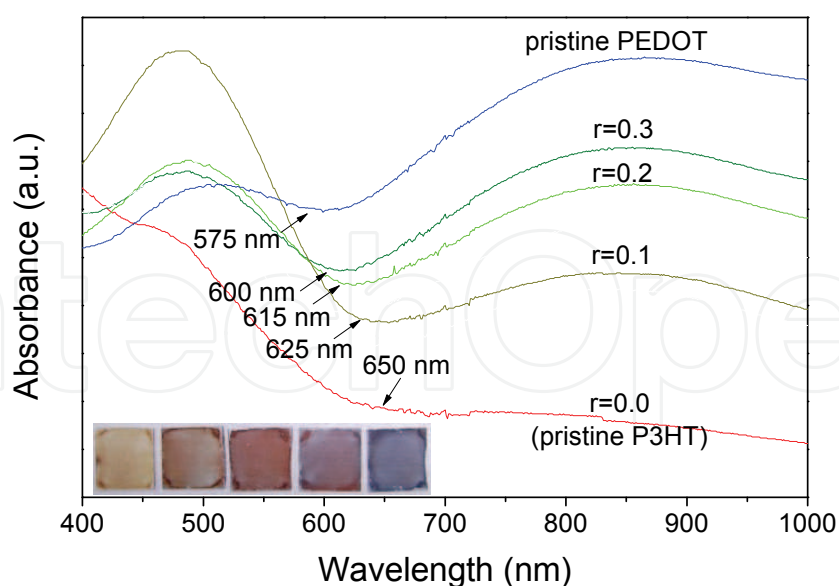


Fig. 3. UV-vis. absorbance spectra of the various PEDOT/P3HT copolymer films. The inset shows pictures of the PEDOT/P3HT copolymer films coated on ITO-coated glass using an oxidant at a 10:1 ratio of mixture to ferric chloride hexahydrate, representing $r = 0, 0.1, 0.2, 0.3, 0.4$, and the pristine PEDOT film from left to right, respectively, with a thickness of 300 nm

6. HOMO of VPP-P3HT

The highest occupied molecular orbital (HOMO) of the VPP-P3HT coating was approximately 5.07 eV (Fig. 4), which is similar to previous studies on organic light-emitting diodes and solar cells. Since the HOMO of P3HT can be adjusted using techniques, such as thermal annealing, the HOMO of the VPP-P3HT in this study can be adjusted for the applications in a variety of optoelectronic devices to meet different electron donor materials.

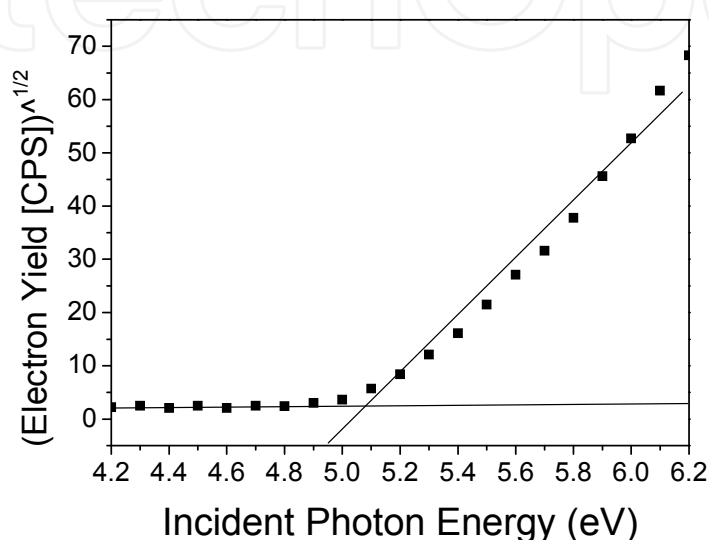


Fig. 4. HOMO (highest occupied molecular orbital) of P3HT thin coating on a ITO-glass substrate

7. Molecular weight and solubility test of VPP-P3HT

7.1 Molecular weight of VPP-P3HT

Determination of the molecular weights of polymers is almost invariably found by gel permeation chromatography (GPC) using polystyrene standards, which indicates relative molecular weights. Conjugation systems such as polythiophenes, however, are known to have a more rod-like conformation in solution, which tends to overestimate the molecular weights of such systems (Holdcroft, 1991). More specifically, in P3HT systems, the molecular weight by GPC is a factor of 1.2 - 2.3 times higher than that by a matrix-assisted laser desorption ionization mass spectrometer (MALDI-MS) (Liu, 1999). Consequently, MALDI-MS was used in this study in order to determine the molecular weight of VPP P3HT. Fig. 5 shows the molecular weight of VPP P3HT measured by MALDI-MS providing peaks at around 994, 1166, and 1333 corresponding to 6 through 8 repeat units of 3-HT (0.74 nm) (Goodman et al., 2009) giving a chain length of 4.44 - 5.92 nm. It is within the effective conjugation length of P3HT (Xu et al., 2007) reported differently in different applications as 9 - 10 thiophene units in polymer light emitting diodes (PLEDs) (Perepichka et al., 2005) and 5 - 7 thiophene units in field effect transistors (FETs) (Johansson & Larsson, 2004). To apply the thin VPP P3HT coatings to many optoelectronic devices, further work will be needed on controlling the molecular weights of VPP P3HT.

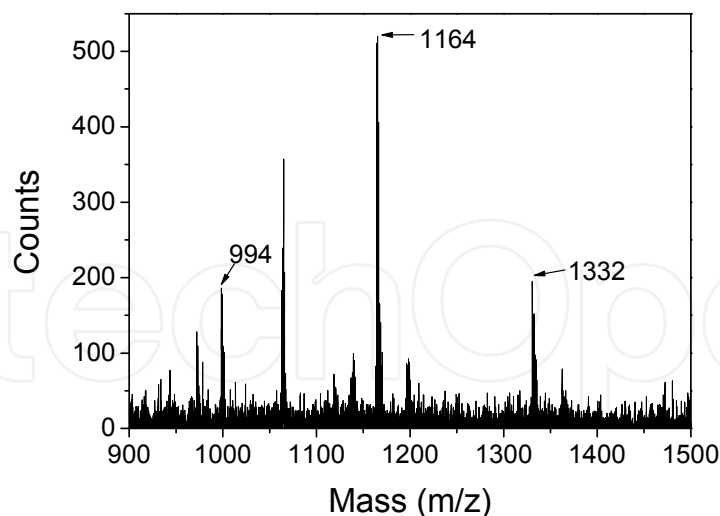


Fig. 5. MALDI-MS spectrum of P3HT vapor-phase polymerized at 55 °C for 1 hour

7.2 Solubility test of VPP-P3HT

Fig. 6 shows the solubility tests of P3HT, monomer (3-HT), and Fe(III) solution demonstrating that the vapor-phase polymerization was successfully carried out in this study. Fig. 6(a) through (c) shows that the VPP P3HT coating (200 nm of thickness in blue color) still remains on the glass as a red-brown layer after being washed with methanol for 3 hours, 1 hour, and 5 min, respectively. As THF is known to be a good solvent of P3HT, Fig. 6(d) shows that the VPP P3HT coating is completely dissolved in THF after 1 min of washing leaving a yellow-colored solution. Although the P3HT is not dissolved in methanol, the Fe(III) or 3-HT monomer is entirely dissolved in methanol. In order to confirm the solubility of the Fe(III) and 3-HT in methanol, the Fe(III) and monomer coatings are shown in Fig. 6(e) and (f) after being washing in methanol for 1 min. As can be seen, these coatings are immediately dissolved in methanol. Consequently, the solubility test proves that P3HT was successfully synthesized by the vapor-phase polymerization in this study because the synthesized P3HT coating remains intact on the glass substrate after thoroughly washed with methanol, which may very well remove unreacted monomers and the Fe(III) from the coating layer.

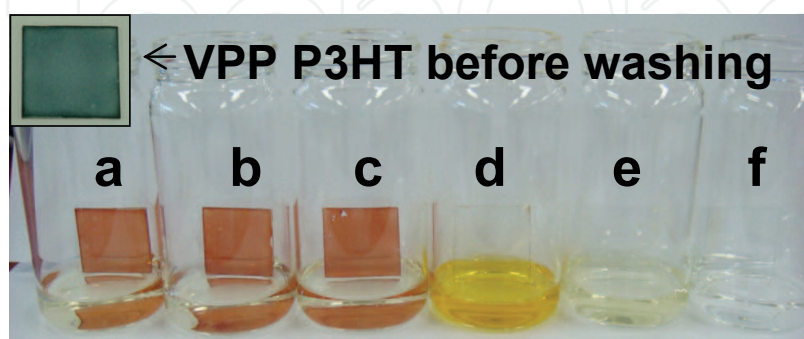


Fig. 6. Solubility test of VPP P3HT coating on glass after being washed with MeOH for 3 hours (a), 1 hour (b), and 5 min (c), and washed with THF for 1 min (d), also exhibiting Fe(III)Cl solution coating (e) and monomers coating (f) on glass after being washed with methanol for 1 min

8. Solvent selection as $\text{Fe(III)Cl}\cdot 6\text{H}_2\text{O}$ solution for fabrication of VPP-P3HT

The surface morphology is important when P3HT is used for thin coating applications because it influences a large number of properties, such as double layer capacitance and adhesion (Truong et al., 2008). It was reported that the polymerization rate of conjugated polymers, surface treatment and Fe(III) solution removal conditions substantially affect the surface morphology of thin film coatings (Truong et al., 2008). For example, B. Winther-Jensen (Winther-Jensen et al., 2004) made a variety of attempts to remove the residual Fe(III)

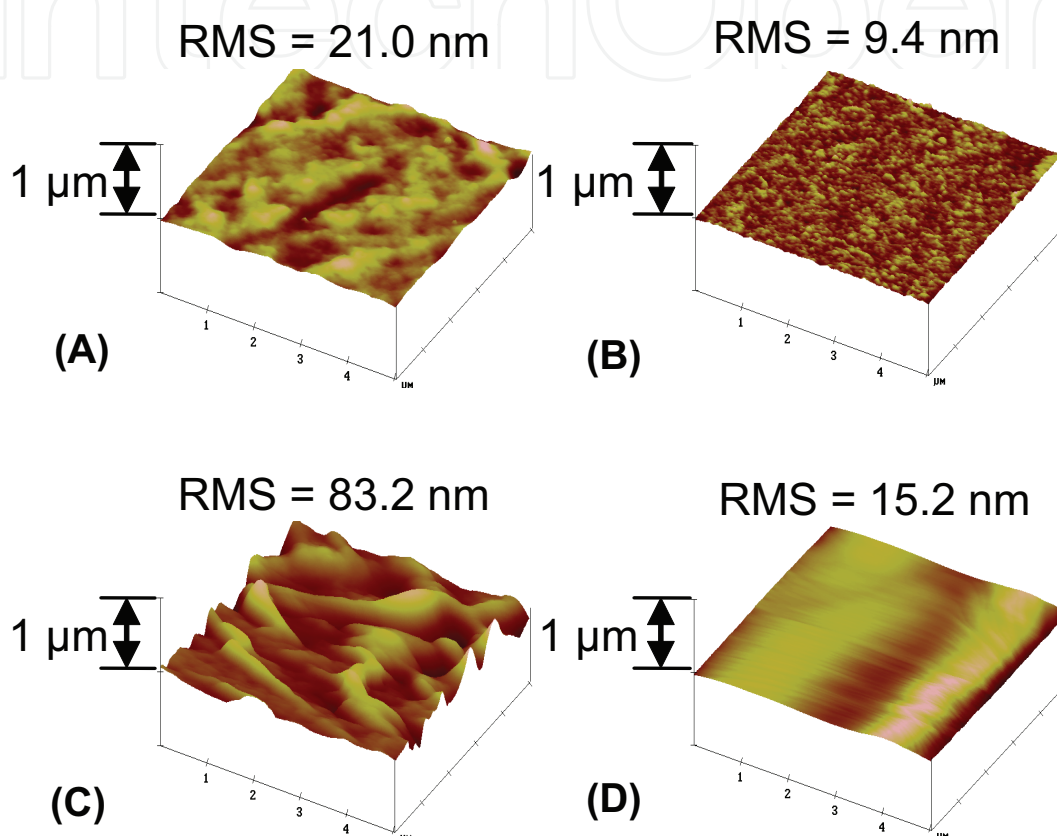


Fig. 7. AFM topography images of the thin P3HT coatings with a $\text{FeCl}_3\cdot 6\text{H}_2\text{O}$ on the glass substrate in cases of a 5% $\text{Fe(III)Cl}\cdot 6\text{H}_2\text{O}$ in EtOH/MeOH (A, before washing; B, after washing), 20% $\text{Fe(III)Cl}\cdot 6\text{H}_2\text{O}$ solution with washing (C), 5% $\text{Fe(III)Cl}\cdot 6\text{H}_2\text{O}$ solution including isopropanol (D)

and monomers successfully in order to make the surfaces of thin conducting polymers smoother. Fig. 7 shows the surface morphology of the P3HT thin coating for different types of solvents for Fe(III) and washing conditions. Fig. 7A and B show the coating surfaces before (A) and after (B) the washing steps for the 5% $\text{FeCl}_3\cdot 6\text{H}_2\text{O}$ in EtOH/MeOH, respectively. The washing process improved the RMS roughness from 21.0 nm to 9.4 nm. In general, the surface roughness of P3HT thin film coatings should not exceed ca. 10 nm for most optoelectronic applications (Truong et al., 2008), which was satisfied in this study. Fig. 7C shows the coating surface after removing the Fe(III) with EtOH/MeOH. The surface roughness of the coating increased with increasing Fe(III) concentration, as shown in Fig. 7B and C, giving a RMS roughness as 9.47 nm and 83.2 nm for the 5% and the 20% $\text{Fe(III)Cl}\cdot 6\text{H}_2\text{O}$ respectively. Although the result is not included

here, the RMS roughness is increased with increasing polymerization time or temperature, mainly due to the increased polymerization rate. It should be noted that other Fe(III)Cl solutions incorporating isopropanol, propanol, or butanol provided produced rougher surfaces than the methanol/ethanol mixture, one of which is shown in Fig. 7D for the isopropanol case. On the other hand, thicker films tend to have higher electric conductivity, which is strongly dependant on the surface roughness. When the thickness of P3HT was more than 300 nm, the surface appeared rougher making it quite difficult to remove the remaining Fe(III) from the coating formed at high concentrations. Moreover, a long polymerization time at low concentration produced a better surface morphology than a short polymerization time at high concentrations, even though the film thicknesses are the same.

9. Experimental demonstration of copolymerization of P3HT and PEDOT

9.1 ATR-FTIR spectra of the PEDOT/P3HT copolymers

The thin copolymers were fabricated by adding a small amount of EDOT monomer in the VPP chamber with excessive 3HT monomers because the polymerization rate of the EDOT monomers was faster than that of the 3HT monomers. More specifically, the composition was controlled by adjusting the feed amount of EDOT to the catalyst-coated layer placed in the reaction chamber, which complies with the typical steady-state plug-flow reactor system (Levenspiel, 1962). In this case, the feed ratio of EDOT to 3HT may be controlled by the inlet size of the vaporized monomers in the stream of purging nitrogen. Simply quantifying the feed composition, the feed ratio (r) may be defined by the feed inlet sizes of EDOT and 3HT, viz: $r = D_{EDOT}/D_{3HT}$, where D_{EDOT} and D_{3HT} are the cross-sectional diameters of the feeding hole on the ceiling of the EDOT and 3HT containers, respectively.

The ATR-FTIR spectroscopy results of the pristine PEDOT, pristine P3HT and PEDOT/P3HT copolymer films are compared in Fig. 8 at different feed ratios. As the characteristic peaks of each pristine polymer, the peak intensity of the aliphatic C-H bond stretching vibration corresponds to the 3-hexyl group in P3HT, and the C-O-C bond stretching vibration corresponds to the ethylenedioxy group in PEDOT. As seen in Fig. 8B, the aliphatic C-H bond stretching in the 3-hexyl group in P3HT appears at 2854, 2924, and 2954 cm^{-1} , and its peak intensity decreases with the feed ratio of r (Chen et al., 1995; Singh et al., 2007). Assigning the bands at approximately 1058 and 1141 cm^{-1} to the stretching modes of the ethylenedioxy group (Zhan et al., 2008; Li et al., 2009), the intensity of these peaks increases with the increasing supply of the EDOT monomer. Consequently, the vapor phase polymerization ratio of PEDOT appears to reflect the controlled supply of the EDOT monomer via the feed ratio of r . Fig. 8C compares the bands of the pristine PEDOT (doped with $\text{FeCl}_3 \cdot 6\text{H}_2\text{O}$) with the copolymers at different feed ratios of r , seemingly exhibiting a redshift due to copolymerization of 3HT and EDOT. The inset in Fig. 8A shows the camera images of pristine PEDOT, P3HT, and PEDOT/P3HT at different compositions coated on the ITO substrates. Since the colors of the pristine PEDOT and P3HT are blue and orange, respectively, the color of the PEDOT/P3HT copolymers changes gradually from orange to dark blue with the increasing EDOT feed ratio of r demonstrating that the ratio was successfully controlled by the feed ratio in our experiments.

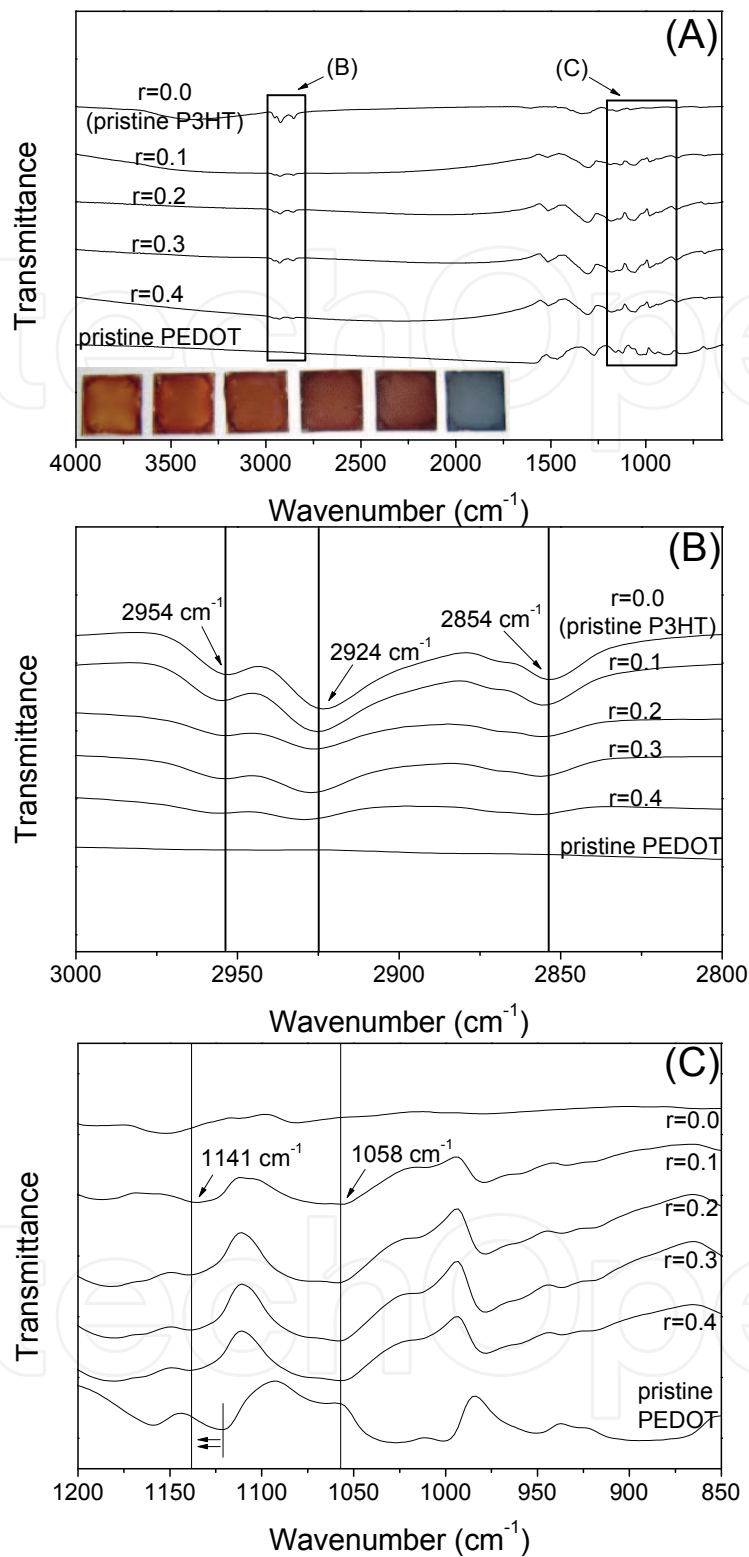


Fig. 8. Comparison of ATR-FTIR spectra of the PEDOT/P3HT copolymers at different feed ratio of r . (A) full spectral region: 4000-600 cm^{-1} , (B) enlargement of the region of 3000-2800 cm^{-1} , (C) enlargement of the region of 1200-850 cm^{-1} . The inset in (A) shows pictures of the PEDOT/P3HT copolymer films coated on ITO-coated glass using an oxidant at a 5:1 ratio of the alcohol mixture to ferric chloride hexahydrate, representing $r = 0, 0.1, 0.2, 0.3, 0.4$, and the pristine PEDOT film from left to right, respectively, with a thickness of 500 nm

9.2 XPS spectra of the PEDOT/P3HT copolymers

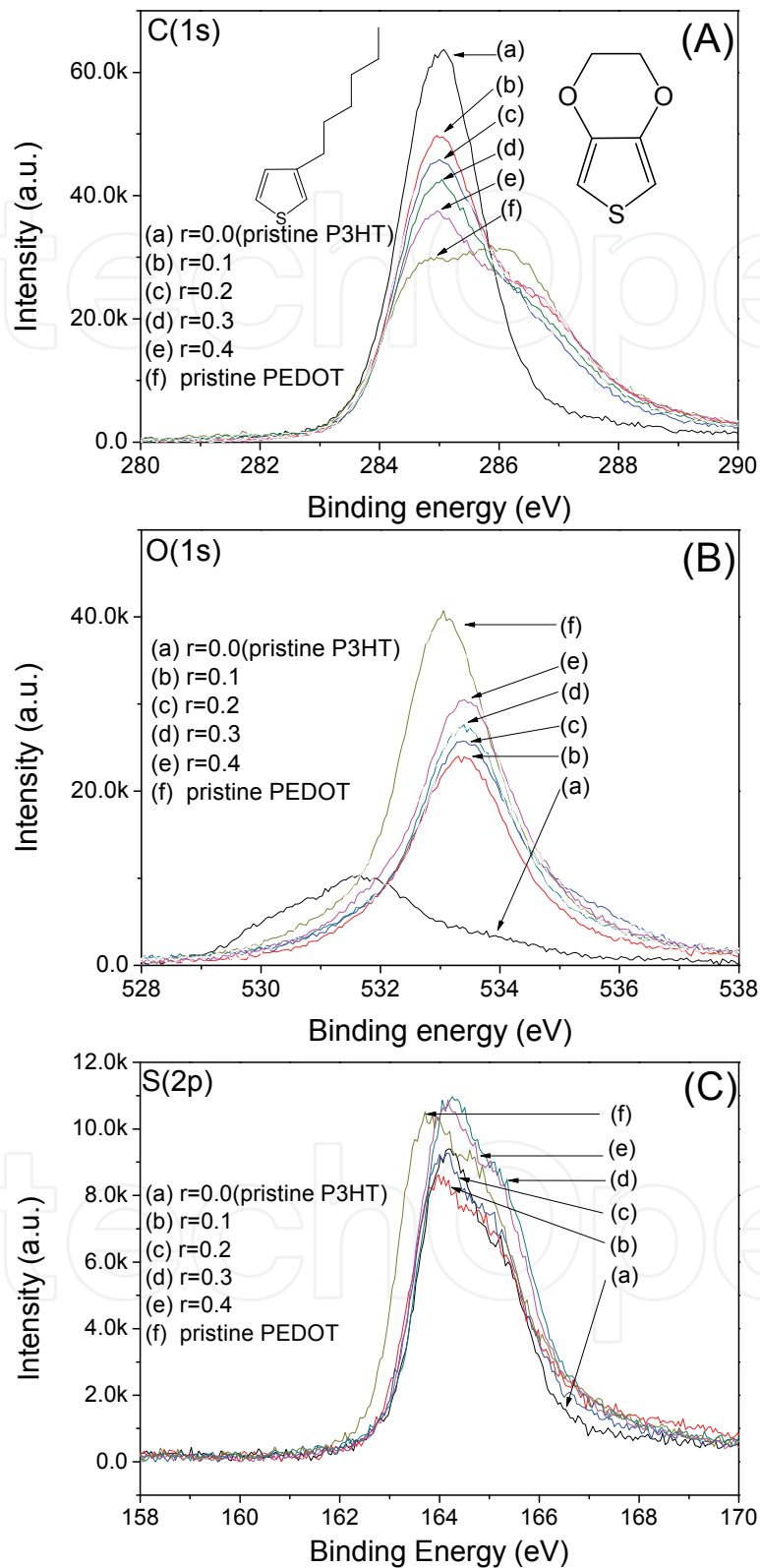


Fig. 9. Deconvolution of XPS spectra of (A) C_(1s), (B) O_(1s) core-level, and (C) S_(2p) for PEDOT/P3HT copolymers at various feed ratio of *r*. The inset in (A) is chemical structures of PEDOT and P3HT, respectively

For copolymers, the surface composition may be quantified using several surface-sensitive techniques, such as XPS and time-of-flight secondary ion mass spectrometry (ToF-SIMS) (Vanden Eynde & Bertrand, 1999), XPS exhibiting somewhat better agreement with the theoretical compositions than ToF-SIMS (Cossement et al., 2006). Therefore, in this study, XPS was used to quantify the surface concentrations. The formation of PEDOT/P3HT copolymer films can be demonstrated by deconvoluting the XPS peaks at 285.0, 286.5, and 533.0 eV, as shown in Fig. 9. The XPS peaks at 285.0 and 286.5 eV in Fig. 9A can be assigned to C-C/C=C and C-O-C, respectively, corresponding to the spectra of the C(1s) core level (Marciniak et al., 2004; Hsiao et al., 2008). Fig. 9A and Table 1 indicate that the intensity of the peak at 285.0 eV decreases with increasing r , whereas that at 286.5 eV increases, which agrees well with the chemical structures of PEDOT and P3HT, as shown in the inset in Fig. 9A. The O photoelectron spectrum in Fig. 9B and Table 1 shows that the O concentration increases with increasing r , as represented by the intensities of the XPS peak at 533 eV, which can be assigned to the oxygen-ether group (C-O-C) (Marciniak et al., 2004; Jonsson et al., 2003). The S photoelectron spectrum is shown in Fig. 9C and analyzed in Table 2.

Samples	C(1s)		h/g
	(g) 285.0 eV (C-C/C=C)	(h) 286.5 eV (C-O-C)	
a	78.4	0	0
b	50.0	24.6	0.49
c	48.1	25.9	0.54
d	42.4	28.4	0.67
e	35.1	28.9	0.82
f	29.2	32.1	1.10

Table 1. XPS atomic concentrations (%) of C and O for PEDOT/P3HT copolymers with (a) $r = 0.0$, (b) 0.1, (c) 0.2, (d) 0.3, (e) 0.4, and (f) pristine PEDOT

Samples	C(1s)	S(2p)	C/S	C/S	PEDOT:P3HT experimental ratio(mol%)
	atom%	atom%	theoretical	experimental	
a	84.1	8.2	10.0	10.3	0:100
b	80.4	8.7	-	9.2	31:69
c	78.4	8.8	-	8.9	39:61
d	75.4	9.7	-	7.8	69:31
e	74.8	9.9	-	7.5	78:22
f	69.5	10.4	6.0	6.7	100:0

Table 2. XPS atomic concentrations (%) of C and S comparing C/S ratios between theoretical and experimental results for (a) $r = 0.0$, (b) 0.1, (c) 0.2, (d) 0.3, (e) 0.4, and (f) pristine PEDOT

The S(2p) peak positions of pristine P3HT and PEDOT appear at 164.1 and 163.8 eV, respectively, and the peaks of their blend systems at different r values seem to appear between the two pristine polymers. Table 2 shows the elemental composition of the fabricated thin films demonstrating that the PEDOT to P3HT ratio increases with the EDOT feed ratio of r . As seen in Table 2, the concentration of S and the PEDOT to P3HT elemental ratio apparently increase with increasing r . Comparing the experimental and theoretical

ratios of C/S, which may represent the ratios of P3HT to PEDOT, there are good agreements between the theoretical and experimental values. The slight discrepancy might be due to adventitious hydrocarbon contamination coming from the contact of the samples with the ambient atmosphere (Cossement et al., 2006).

10. Electrical and surface properties of the pristine PEDOT, P3HT, and PEDOT/P3HT copolymer films

10.1 Electrical conductivities

Fig. 10 shows the electrical conductivity of the copolymers plotted as a function of r . The electrical conductivity increases from 3.0×10^{-2} S/cm for the pristine P3HT up to 6.28 S/cm for the copolymer with r at 0.4. The conductivity of PEDOT/P3HT copolymer can be increased up to 200 times higher than that of the pristine P3HT, which can be achieved by adjusting the EDOT feed ratio of r . In this study, the conductivity of the pristine VPP-PEDOT was similar to that reported elsewhere (Kim et al., 2003), where a FeCl_3 -based oxidant solution was used without any additives. However, the addition of basic inhibitors, such as pyridine (Winther-Jensen et al., 2004) and imidazole (Ha et al., 2004), has been reported to reduce the polymerization reaction kinetics and enhance the conductivity and transparency of the PEDOT film. Therefore, a weak base can be used to the PEDOT/P3HT copolymer systems to achieve high conductivities, which is desirable for electrode systems in various electronic devices.

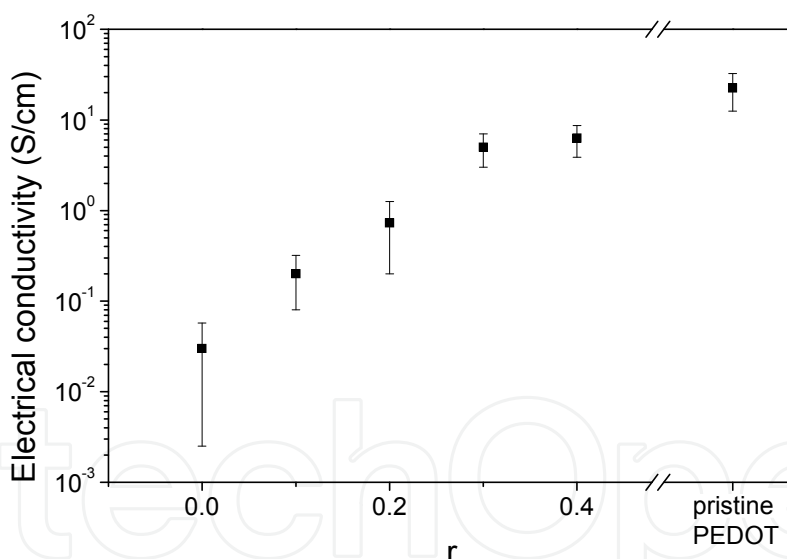


Fig. 10. Electrical conductivities of the pristine PEDOT, P3HT, and PEDOT/P3HT copolymer films

10.2 Water contact angles and RMS surface roughness

Fig. 11 shows the water contact angle and RMS surface roughness of the copolymerized films coated on the glass substrates. Since a liquid makes contact with the outermost molecular layer of a surface, the contact angles represent the chemical and structural differences at the coating surface. Furthermore, the wettability of the thin coating is important in the fabrication of many optoelectronic devices, where multilayers should be fabricated in contact with heterogeneous layers. Since the contact angle of the pristine

PEDOT at 36° is lower than that of the pristine P3HT at 54° , the PEDOT/P3HT copolymer films show a decreasing feature of the contact angle with a higher r , which is likely affected by the roughness of the coating since the water contact angle usually decreases with increasing RMS roughness. At a feed ratio of $r = 0.4$, however, the contact angle is slightly lower than the pristine PEDOT. Exhibited by the camera images of coating in the insets of Fig. 11, the color changes gradually from yellow to blue with the increasing EDOT feed ratio of r .

Overall, the developed VPP copolymerizing technique clearly demonstrates that the physicochemical properties of PEDOT/P3HT copolymers were successfully adjusted. Since the vapor pressure and polymerization rates of EDOT and 3HT monomers are different, the variation of the copolymer composition was ensured by adjusting the feed ratio of the monomers to the reaction chamber, which resulted in different reactant concentrations of EDOT and 3HT monomers. Different concentrations of reactants may well give different kinetic polymerization rates of EDOT and 3HT to provide a controllable synthesis route of PEDOT/P3HT copolymer coatings. Further study should be performed to identify the detailed copolymerization reaction and chemical structures of the VPP PEDOT/P3HT copolymer system.

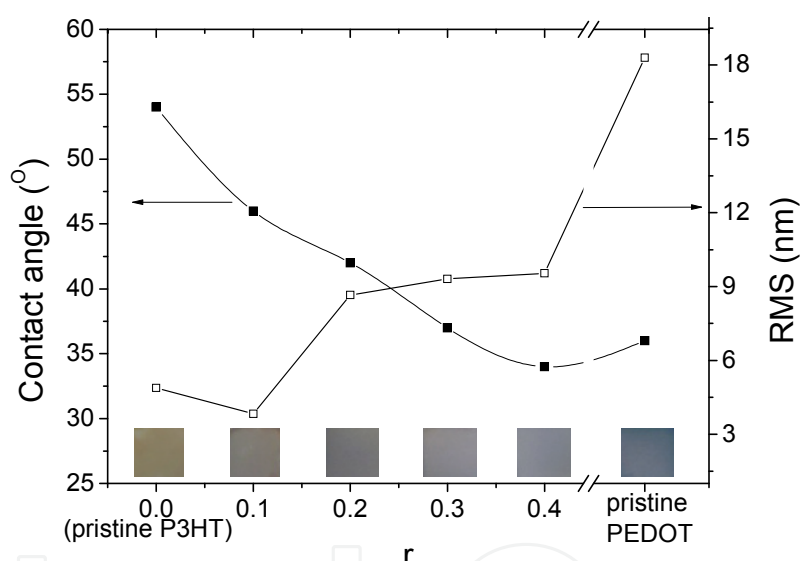


Fig. 11. Water contact angles and RMS surface roughness for different PEDOT/P3HT films. The inset shows the camera images of PEDOT/P3HT copolymer films with thickness of ca. 100 nm

11. Conclusion

A conducting thin P3HT coating was successfully fabricated on various substrates with a thickness ranging from 50 nm to 1 μm by vapor phase polymerization of a 3HT monomer. The most appropriate Fe(III) solution was found to be 5 % $\text{FeCl}_3 \cdot 6\text{H}_2\text{O}$ in MeOH/EtOH (1:1) providing good conductivity ($10^{-2} \sim 10^{-4}$ S/cm) and transmittance (< 91 %). The RMS roughness of VPP-P3HT was 9.4 nm. The band gap and HOMO of VPP-P3HT were found to be 1.91 eV (650 nm) and 5.07 eV, respectively, which may be suitable for applications in optoelectronic devices. For further study, PEDOT/P3HT copolymer films were also successfully fabricated as thin films on the glass, Si wafer, ITO-covered glass and PET film

substrates using a vapor phase polymerization technique. The ratios were kinetically controlled to ensure the tunable properties of bandgap, electrical conductivity, surface morphology and water contact angle of the thin copolymer films. The P3HT thin film incorporated with PEDOT may improve the mobility in OTFTs and charge extraction efficiency in OPVs. In addition to being used as a semiconductor with higher mobility, adding dopants to increase the electrical conductivity, P3HT/PEDOT copolymer films can also be used as a HIL in OLEDs with modified energy levels and properties.

12. References

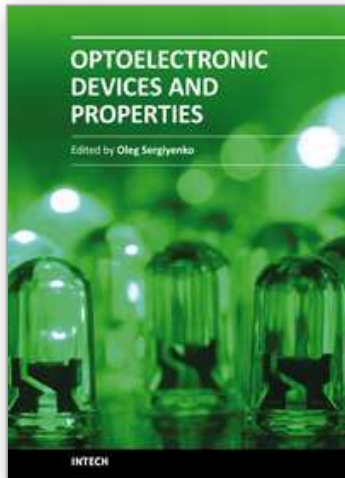
- Admassie, S.; Zhang, F.; Manoj, A.; Svensson, M.; Andersson, M.; Inganas, O. (2006). A polymer photodiode using vapour-phase polymerized PEDOT as an anode *Sol. Energ. Mat. Sol. C.* 90, 133-141.
- Bartic, C.; Jansen, H.; Campitelli, A.; Borghs, S. (2002). Ta₂O₅ as gate dielectric material for low-voltage organic thin-film transistors *Org. Electron.* 3, 65-72.
- Chan, H. S. O.; Ng, S. C. (1998). Synthesis, characterization and applications of thiophene-based functional polymers *Prog. Polym. Sci.* 23, 1167.
- Chen, T. A.; Wu, X.; Rieke, R. D. (1995). Regiocontrolled Synthesis of Poly(3-alkylthiophenes) Mediated by Rieke Zinc: Their Characterization and Solid-State Properties *J. Am. Chem. Soc.* 117, 233.
- Chen, T.; Wu, X.; Rieke, R. (1995). Regiocontrolled Synthesis of Poly(3-alkylthiophenes) Mediated by Rieke Zinc: Their Characterization and Solid-State Properties *J. Am. Chem. Soc.* 117, 233-244.
- Chiang, C.K.; Fincher, C.R.; Park, Y.W.; Heeger, A.; Shirakawa, H.; Louis, E.J.; Gau, S.C.; MacDiarmid A.G. (1977). Electrical Conductivity in Doped Polyacetylene *Phys. Rev. Lett.* 39, 1098-1101
- Cho, M.; Kim, S.; Nam, J.; Lee, Y. (2008). Preparation of PEDOT/Cu composite film by in situ redox reaction between EDOT and copper(II) chloride *Synthetic Met.* 158, 865-869.
- Colladet, K.; Fourier, S.; Cleij, T.; Lutsen, L.; Gelan, J.; Vanderzande, D.; Neugebauer, H.; Sariciftci, S.; Aguirre, A.; Janssen, G. (2007). Low Band Gap Donor-Acceptor Conjugated Polymers toward Organic Solar Cells Applications *Macromolecules* 40, 65-72.
- Du Pasquier, A.; Unalan, H. E.; Kanwal, A.; Miller, S.; Chhowalla, M. (2005). Conducting and transparent single-wall carbon nanotube electrodes for polymer-fullerene solar cells *Appl. Phys. Lett.* 87, 203511.
- Fabretto, M.; Zuber, K.; Hall, C.; Murphy, P. (2008). High Conductivity PEDOT Using Humidity Facilitated Vacuum Vapour Phase Polymerisation *Macromol. Rapid Comm.* 29, 1403-1409.
- Gadisa, A.; Tvingstedt, K.; Admassie, S.; Lindell, L.; Crispin, X.; Andersson, M.; Salaneck, W.; Inganas, O. (2006). Transparent polymer cathode for organic photovoltaic devices *Synthetic Met.* 156, 1102-1107.
- Goodman, M. D.; Xu, J.; Wang, J.; Lin, Z. (2009). Semiconductor Conjugated Polymer-Quantum Dot Nanocomposites at the Air/Water Interface and Their Photovoltaic Performance *Chem. Mater.* 21, 934
- Greco, S.; Roggenbuck, M.; Opitz, A.; Brutting, W. (2006). Differences of interface and bulk transport properties in polymer field-effect devices *Org. Electron.* 7, 276-286.

- Groenendaal, L.; Jonas, F.; Freitag, D.; Pielartzik, H.; Reynolds, J. (2000). Poly(3,4-ethylenedioxythiophene) and Its Derivatives: Past, Present, and Future *Adv. Mater.* 12, 481-494.
- Groenendaal, L.; Zotti, G.; Jonas, G. (2001). Optical, conductive and magnetic properties of electrochemically prepared alkylated poly(3,4-ethylenedioxythiophene)s *Synthetic Met.* 118, 105-109.
- Ha, Y.; Nikolov, N.; Pollack, S.; Mastrangelo, J.; Martin, B.; Shashidhar, R. (2004). Towards a Transparent, Highly Conductive Poly(3,4-ethylenedioxythiophene) *Adv. Funct. Mater.* 14, 615-622.
- Hatton, R.; Blanchard, N.; Tan, L.; Latini, G.; Cacialli, F.; Silva, S. (2009). Oxidised carbon nanotubes as solution processable, high work function hole-extraction layers for organic solar cells *Org. Electron.* 10, 388-395.
- Higgins, A.; Martin, S.; Jukes, P.; Geoghegan, M.; Jones, R.; Langridge, S.; Cubitt, R.; Kirchmeyer, S.; Wehrum, A.; Grizzi, I. (2003). Interfacial structure in semiconducting polymer devices *J. Mater. Chem.* 13, 2814-2818.
- Holdcroft, S. J. (1991). Determination of molecular weights and Mark-Houwink constants for soluble electronically conducting polymers *Polym. Sci., Part B.* 29, 1585.
- Jang, K.; Eom, Y.; Lee, T.; Kim, D.; Oh, Y.; Jung, H.; Nam, J. (2009). Fabrication of Poly(3-hexylthiophene) Thin Films by Vapor-Phase Polymerization for Optoelectronic Device Applications *ACS Appl. Mater. Interfaces* 1, 1567-1571.
- Jang, K.; Kim, D.; Lee, J.; Hong, S.; Lee, T.; Lee, Y.; Nam, J. (2010). Synchronous vapor-phase polymerization of poly(3,4-ethylenedioxythiophene) and poly(3-hexylthiophene) copolymer systems for tunable optoelectronic properties *Org. Electron.* 11, 1668-1675.
- Johansson, E. & Larsson, S. (2004). Electronic structure and mechanism for conductivity in thiophene oligomers and regioregular polymer *Synthetic Met.* 144, 183
- Jonas, F.; Schrader, L. (1991). Conductive modifications of polymers with polypyrroles and polythiophenes *Synthetic Met.* 41, 831-836.
- Kemerink, M.; Timpanaro, S.; De Kok, M.; Meulenkaamp, E.; Touwslager, F. (2004). Three-Dimensional Inhomogeneities in PEDOT:PSS Films *J. Phys. Chem. B* 108, 18820-18825.
- Kim, D.; Lee, L.; Kang, S.; Jang, K.; Lee, J.; Cho, M.; Nam, J. (2009). In-situ blends of polypyrrole/poly(3,4-ethylenedioxythiophene) using vapor phase polymerization technique *Thin Solid Films* 517, 4156-4160.
- Kim, J.; Kim, E.; Won, Y.; Lee, H.; Suh, K. (2003). The preparation and characteristics of conductive poly(3,4-ethylenedioxythiophene) thin film by vapor-phase polymerization *Synthetic Met.* 139, 485-489.
- Kim, Y.; Choulis, S.; Nelson, J.; Bradley, D.; Cook, S.; Durrant, J. (2005). Device annealing effect in organic solar cells with blends of regioregular poly(3-hexylthiophene) and soluble fullerene *Appl. Phys. Lett.* 86, 063502.
- Lee, T. & Chung, Y. (2008). Control of the Surface Composition of a Conducting-Polymer Complex Film to Tune the Work Function *Adv. Funct. Mater.* 18, 2246-2252.
- Lee, T.; Chung, Y.; Kwon, O.; Park, J. (2007). Self-Organized Gradient Hole Injection to Improve the Performance of Polymer Electroluminescent Devices *Adv. Funct. Mater.* 17, 390-396.
- Levenspiel, O. (1962). Chemical reaction engineering, John Wiley and Sons, New York, 1962

- Li, L.; Huang, Y.; Yan, G.; Liu, F.; Huang, Z.; Ma, Z. (2009). Poly(3,4-ethylenedioxythiophene) nanospheres synthesized in magnetic ionic liquid *Mater. Lett.* 63, 8-10.
- Li, Z. L.; Yang, S. C.; Meng, H. F.; Chen, Y. S.; Yang, Y. Z.; Liu, C. H.; Horng, S. F.; Hsu, C. S.; Chen, L. C.; Hu, J. P. (2004). Patterning-free integration of polymer light-emitting diode and polymer transistor *Appl. Phys. Lett.* 84, 3558
- Liu, J.; Loewe, R. S.; McCullough, R. D. (1999). Employing MALDI-MS on Poly(alkylthiophenes): Analysis of Molecular Weights, Molecular Weight Distributions, End-Group Structures, and End-Group Modifications *Macromolecules* 32, 5777
- McCullough, R. D. (1998). The Chemistry of Conducting Polythiophenes *Adv. Mat.* 10, 93.
- Perepichka, I. F.; Perepichka, D. F.; Meng, H.; Wudl, F. (2005). Light-Emitting Polythiophenes *Adv. Mat.* 17, 2281.
- Saito, Y.; Kitamura, T.; Wada, Y.; Yanagida, S. (2002). Poly(3,4-ethylenedioxythiophene) as a hole conductor in solid state dye sensitized solar cells *Synthetic Met.* 131, 185-187.
- Sarac, A.; Sonmez, G.; Cebeci, F. (2003). Electrochemical synthesis and structural studies of polypyrroles, poly(3,4-ethylene-dioxythiophene)s and copolymers of pyrrole and 3,4-ethylenedioxythiophene on carbon fibre microelectrodes *J. Appl. Electrochem.* 33, 295-301.
- Shirakawa, H.; Louis E.; MacDiarmid, A.; Chiang, C.; Heeger, A. (1977). Synthesis of electrically conducting organic polymers: halogen derivatives of polyacetylene, (CH)_x *J. S. C., Chem. Commun.* 1977, 578-580
- Singh, R.; Kumar, J.; Singh, R.; Kant, R.; Chand, S.; Kumar, V. (2007). Micromorphology, photophysical and electrical properties of pristine and ferric chloride doped poly(3-hexylthiophene) films *Mater. Chem. Phys.* 104, 390-396.
- Skotheim, T. A.; Reynolds, J. R. Eds.; Handbook of conducting polymers, CRS press 2007.
- Terje A. Skotheim, Handbook of Conducting Polymer Marcel Dekker, New york, 1998.
- Truong, T.; Kim, D.; Lee, Y.; Lee, T.; Park, J.; Pu, L.; Nam, J. (2008). Surface smoothness and conductivity control of vapor-phase polymerized poly(3,4-ethylenedioxythiophene) thin coating for flexible optoelectronic applications *Thin Solid Films* 516, 6020-6027.
- Wakizaka, D.; Fushimi, T.; Ohkita, H.; Ito, S. (2004). Hole transport in conducting ultrathin films of PEDOT/PSS prepared by layer-by-layer deposition technique *Polymer* 45, 8561-8565.
- Welsh, D.; Kumar, A.; Meijer, E.; Reynolds, J. (1999). Enhanced Contrast Ratios and Rapid Switching in Electrochromics Based on Poly(3,4-propylenedioxythiophene) Derivatives *Adv. Mater.* 11, 1379-1382.
- Winther-Jensen, B.; Chen, J.; West, K.; Wallace, G. (2004). Vapor Phase Polymerization of Pyrrole and Thiophene Using Iron(III) Sulfonates as Oxidizing Agents *Macromolecules* 37, 5930.
- Winther-Jensen, B.; Chen, J.; West, K.; Wallaces, G. (2004). Vapor Phase Polymerization of Pyrrole and Thiophene Using Iron(III) Sulfonates as Oxidizing Agents *Macromolecules* 37, 5930-5935.
- Winther-Jensen, B.; Forsyth, M.; West, K.; Andreasen, J.; Wallace, G.; MacFarlane, D. (2007). High current density and drift velocity in templated conducting polymers *Org. Electron.* 8, 796-800.

- Winther-Jensen, B.; West, K. (2004). Vapor-Phase Polymerization of 3,4-Ethylenedioxythiophene: A Route to Highly Conducting Polymer Surface Layers *Macromolecules* 37, 4538-4543.
- Xu, J.; Wang, J.; Mitchell, M.; Mukherjee, P.; Jeffries-EL, M.; Petrich, J. W.; Lin, Z. (2007). Organic-Inorganic Nanocomposites via Directly Grafting Conjugated Polymers onto Quantum Dots *J. Am. Chem. Soc.* 129, 12828
- Xu, Y.; Wang, J.; Sun, W.; Wang, S. (2006). Capacitance properties of poly(3,4-ethylenedioxythiophene)/polypyrrole composites *J. Power Sources* 159, 370-373.
- Zhan, L.; Song, Z.; Zhang, J.; Tang, J.; Zhan, H.; Zhou, Y.; Zhan, C. (2008). PEDOT: Cathode active material with high specific capacity in novel electrolyte system *Electrochim. Acta* 53, 8319-8323.

IntechOpen



Optoelectronic Devices and Properties

Edited by Prof. Oleg Sergiyenko

ISBN 978-953-307-204-3

Hard cover, 660 pages

Publisher InTech

Published online 19, April, 2011

Published in print edition April, 2011

Optoelectronic devices impact many areas of society, from simple household appliances and multimedia systems to communications, computing, spatial scanning, optical monitoring, 3D measurements and medical instruments. This is the most complete book about optoelectromechanic systems and semiconductor optoelectronic devices; it provides an accessible, well-organized overview of optoelectronic devices and properties that emphasizes basic principles.

How to reference

In order to correctly reference this scholarly work, feel free to copy and paste the following:

Keon-Soo Jang and Jae-Do Nam (2011). Synchronous Vapor-Phase Coating of Conducting Polymers for Flexible Optoelectronic Applications, Optoelectronic Devices and Properties, Prof. Oleg Sergiyenko (Ed.), ISBN: 978-953-307-204-3, InTech, Available from: <http://www.intechopen.com/books/optoelectronic-devices-and-properties/synchronous-vapor-phase-coating-of-conducting-polymers-for-flexible-optoelectronic-applications>

INTECH
open science | open minds

InTech Europe

University Campus STeP Ri
Slavka Krautzeka 83/A
51000 Rijeka, Croatia
Phone: +385 (51) 770 447
Fax: +385 (51) 686 166
www.intechopen.com

InTech China

Unit 405, Office Block, Hotel Equatorial Shanghai
No.65, Yan An Road (West), Shanghai, 200040, China
中国上海市延安西路65号上海国际贵都大饭店办公楼405单元
Phone: +86-21-62489820
Fax: +86-21-62489821

© 2011 The Author(s). Licensee IntechOpen. This chapter is distributed under the terms of the [Creative Commons Attribution-NonCommercial-ShareAlike-3.0 License](#), which permits use, distribution and reproduction for non-commercial purposes, provided the original is properly cited and derivative works building on this content are distributed under the same license.

IntechOpen

IntechOpen